

1
2
3
4
5
6
7
8
9
10
11
12
13
14
15
16
17
18
19
20
21
22
23
24
25
26
27
28
29
30
31
32

Human genetic analyses of organelles highlight the nucleus in age-related trait heritability

Rahul Gupta^{1,2,3}, Konrad J. Karczewski^{2,3}, Daniel Howrigan^{2,3}, Benjamin M. Neale^{2,3,*}, Vamsi K. Mootha^{1,2,*}

¹ Howard Hughes Medical Institute and Department of Molecular Biology, Massachusetts General Hospital, Boston, MA 02114

² Broad Institute of MIT and Harvard, Cambridge, MA 02142

³ Analytic and Translational Genetics Unit, Center for Genomic Medicine, Massachusetts General Hospital, Boston, MA 02114, USA

*Corresponding authors: bneale@broadinstitute.org (B.M.N.), vamsi@hms.harvard.edu (V.K.M.)

Keywords: mitochondria, nucleus, aging, oxidative phosphorylation, OXPHOS, transcription factor, zinc finger, KRAB domain, gene regulation, UK Biobank, constraint, dominance, haplosufficiency, haplosufficient, PPARGC1A, ESRRB, TFAM

33 **Abstract**

34 Aging is associated with defects in many organelles, but an open question is whether the inherited risk for
35 age-related disease is enriched within loci relevant to each organelle. Here, we begin with a focus on
36 mitochondria, as mitochondrial dysfunction is a hallmark of age-related disease. We report a striking lack
37 of enrichment of mitochondria-relevant loci across GWAS for 24 age-related traits. Analyses of nine
38 additional organelles reveal enrichment only for the nucleus, particularly nuclear transcription factors.
39 Consistent with these results, natural selection appears to exert stronger purifying selection against
40 protein-truncating variants for transcription factors compared to mitochondrial pathways, underscoring
41 the importance of inherited variation in gene-regulation in age-related traits.

42

43 **Introduction**

44 The global burden of age-related diseases such as type 2 diabetes (T2D), Parkinson’s disease (PD), and
45 cardiovascular disease (CVD) has been steadily rising due in part to a progressively aging population. These
46 diseases are often highly heritable¹. Genome-wide association studies (GWAS) have led to the discovery
47 of thousands of robust associations with common genetic variants², implicating a complex genetic
48 architecture as underlying much of the heritable risk. These loci hold the potential to reveal underlying
49 mechanisms of disease and spotlight targetable pathways.

50 Aging has been associated with dysfunction in many cellular organelles. This is perhaps most notable for
51 the mitochondria, dysfunction in which is frequently invoked as a key “hallmark” of aging³ and has been
52 nominated as a candidate driver of virtually all common age-associated diseases. In particular, deficits in
53 mitochondrial oxidative phosphorylation (OXPHOS), the chief pathway for ATP production, is often
54 observed in these diseases as evidenced by a decline in *in vivo* ³¹P-NMR measures of OXPHOS activity^{4,5}, a
55 decline in electron transport chain enzymatic activity^{6–12} in biopsy/autopsy material, an accumulation of
56 somatic mtDNA mutations^{13–15}, and a decline in mtDNA copy number (mtCN)¹⁶. Protein products from
57 both the nuclear DNA (nucDNA), which encodes ~1100 proteins that primarily localize to the
58 mitochondria¹⁷, and the mitochondrial DNA (mtDNA), which encodes 13 proteins, are critical for proper
59 OXPHOS homeostasis¹⁸. Rare, inherited mutations in any of ~300 nucDNA or mtDNA genes can cause
60 severe “primary” mitochondrial diseases that impact multiple organ systems¹⁹. Dysfunction in other
61 organelles³, such as the nucleus (e.g., increased gene regulatory noise from epigenetic alterations³,
62 telomere shortening^{20,21}), the lysosome²², and the endoplasmic reticulum²³, has also been associated with
63 aging and/or age-related disease.

64 A key question is whether inherited variation influencing organelle function is enriched for age-related
65 disease risk. In the present study, we use a human genetics approach to assess common variation in loci
66 relevant to the function of 10 cellular organelles. We begin with a deliberate focus on mitochondria given
67 the depth of literature linking it to age-related disease, testing nucDNA and mtDNA loci relevant for
68 mitochondrial function in 24 different age-related diseases and traits. We hypothesized that heritability
69 for common, age-related traits would be overrepresented among mitochondria-relevant loci, namely
70 variants near genes encoding the organelle’s proteome or loci associated with quantitative readouts of
71 mitochondrial function.

72 To our surprise, we find no evidence of enrichment for genome-wide association signal in mitochondria-
73 relevant loci across any of our analyses. Of ten tested organelles, only the nucleus shows enrichment
74 among many age-associated traits, with the signal emanating from the transcription factors. Further
75 analysis shows that genes encoding the mitochondrial proteome tend to be tolerant to heterozygous
76 predicted loss-of-function (pLoF) variation and thus are surprisingly “haplosufficient,” whereas nuclear
77 transcription factors are especially sensitive to gene dosage and are often “haploinsufficient”. Thus, we
78 highlight variation influencing gene-regulatory pathways, rather than organelle physiology, in the
79 inherited risk of common age-associated diseases.

80 **Results**

81 **Age-related diseases and traits show diverse genetic architectures**

82 To systematically define age-related diseases, we turned to recently published epidemiological data from
83 the United Kingdom (U.K.)²⁴ in order to match the U.K. Biobank (UKB)²⁵ cohort. We prioritized traits whose
84 prevalence increased as a function of age (**Methods**) and were represented in UKB
85 (https://github.com/Nealelab/UK_Biobank_GWAS) and/or had available published GWAS meta-
86 analyses^{26–35} (**Figure 1A, Supplementary note**). We used SNP heritability estimates from stratified linkage
87 disequilibrium score regression (S-LDSC, <https://github.com/bulik/ldsc>)³⁶ to ensure that our selected traits
88 were sufficiently heritable (**Methods, Supplementary note**). We then computed pairwise genetic

89 correlations between the age-associated traits to compare their respective genetic architectures (**Figure**
 90 **1B**, **Table S2**, **Methods**). As expected we find a highly correlated module of primarily cardiometabolic
 91 traits with high density lipoprotein (HDL) showing anti-correlation³⁷. Interestingly, several other traits
 92 (gastroesophageal reflux disease (GERD), osteoarthritis) showed moderate correlation to the
 93 cardiometabolic trait cluster while atrial fibrillation, for which T2D and CVD are risk factors³⁸, did not. Our
 94 final set of prioritized, age-associated traits included 24 genetically diverse, heritable phenotypes (**Table**
 95 **S1**). Of these, 11 traits were sufficiently heritable only in UKB, 3 were sufficiently heritable only among
 96 non-UKB meta-analyses, and 10 were well-powered in both UKB and an independent cohort.

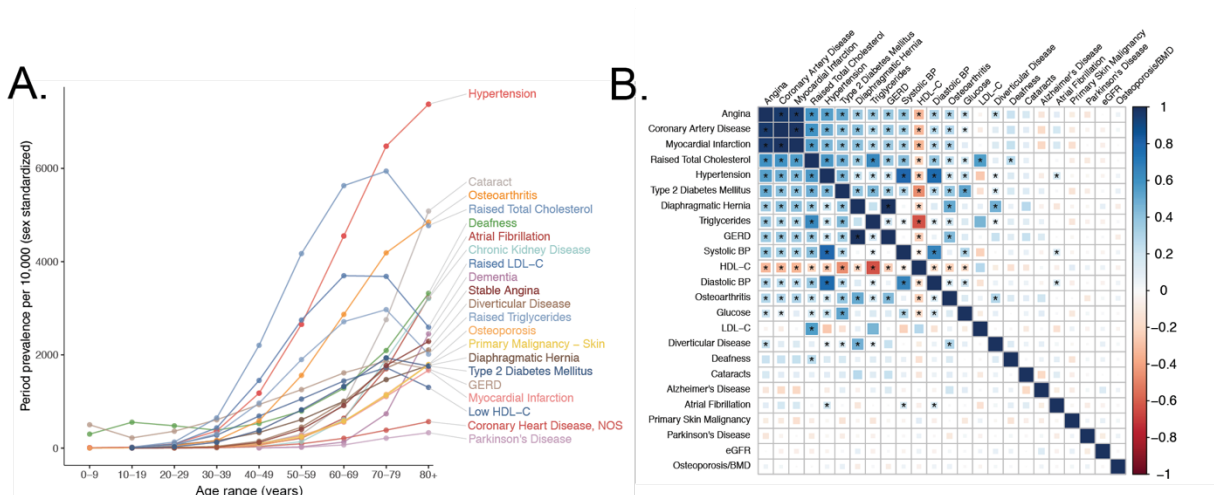


Figure 1. Selection of genetically diverse age-related diseases and traits using epidemiological data. **A.** Period prevalence of age-associated diseases systematically selected for this study (**Methods**). Epidemiological data obtained from Kuan et al. 2019. **B:** Genetic correlation between the selected age-related traits. All correlations were assessed between UK Biobank phenotypes with the exception of eGFR, Alzheimer's Disease, and Parkinson's Disease, for which the respective meta-analyses were used (**Methods**). Point estimates and standard errors reported in **Table S2**. * represent genetic correlations that are significantly different from 0 at a Bonferroni-corrected threshold for $p = 0.05 \times 24$ traits.

97
 98 **No evidence for enrichment of age-related trait heritability in mitochondria-relevant loci**
 99 To test if age-related trait heritability was enriched among mitochondria-relevant loci, we began by simply
 100 asking if ~1100 nucDNA genes encoding the mitochondrial proteome from the MitoCarta2.0 inventory¹⁷
 101 were found near lead SNPs for our selected traits represented in the NHGRI-EBI GWAS Catalog
 102 (<https://www.ebi.ac.uk/gwas/>)³⁹ more frequently than expectation (**Methods, Supplementary note**). To
 103 our surprise, no traits showed a statistically significant enrichment of mitochondrial genes (**Figure S1A**);
 104 in fact, six traits showed a statistically significant depletion. Even more strikingly, MitoCarta genes tended
 105 to be nominally enriched in fewer traits than the average randomly selected sample of protein-coding
 106 genes (**Figure S1B**, empirical $p = 0.014$). This lack of enrichment was observed more broadly across
 107 virtually all traits represented in the GWAS Catalog (**Figure S1C**). We also tested several transcriptional
 108 regulators of mitochondrial biogenesis and function – *TFAM*, *GABPA*, *GABPB1*, *ESRRA*, *YY1*, *NRF1*,
 109 *PPARGC1A*, *PPARGC1B*. We found little evidence supporting a role for these genes in modifying risk for
 110 the age-related GWAS Catalog phenotypes, observing only a single trait (heel bone mineral density) for
 111 which a mitochondrial transcriptional regulator (*TFAM*) was nearest an associated genome-wide
 112 significant variant (**Supplementary note**).

113 To investigate further, we turned to U.K. Biobank (UKB). We compiled and tested three classes of
 114 “mitochondria-relevant loci” (**Figure 2A**) with which we interrogated the association between common
 115 mitochondrial variation and common disease. First, we curated literature-reported nucDNA quantitative
 116 trait loci (QTLs) associated with measures of mitochondrial function (**Table S3**): mtCN^{40,41}, mtRNA

117 abundance and modification^{42,43}, and plasma levels of OXPHOS dysfunction biomarkers including GDF15
 118 protein^{44,45}, lactate, pyruvate, and lactate/pyruvate ratio⁴⁶⁻⁴⁸. Second, we considered all common variants
 119 in or near nucDNA MitoCarta genes, as well as two subsets of MitoCarta: mitochondrial Mendelian disease
 120 genes¹⁹ and nucDNA-encoded OXPHOS genes. Third, we obtained mtDNA genotypes at up to 213 loci after
 121 quality control (**Methods**) from 360,662 individuals.

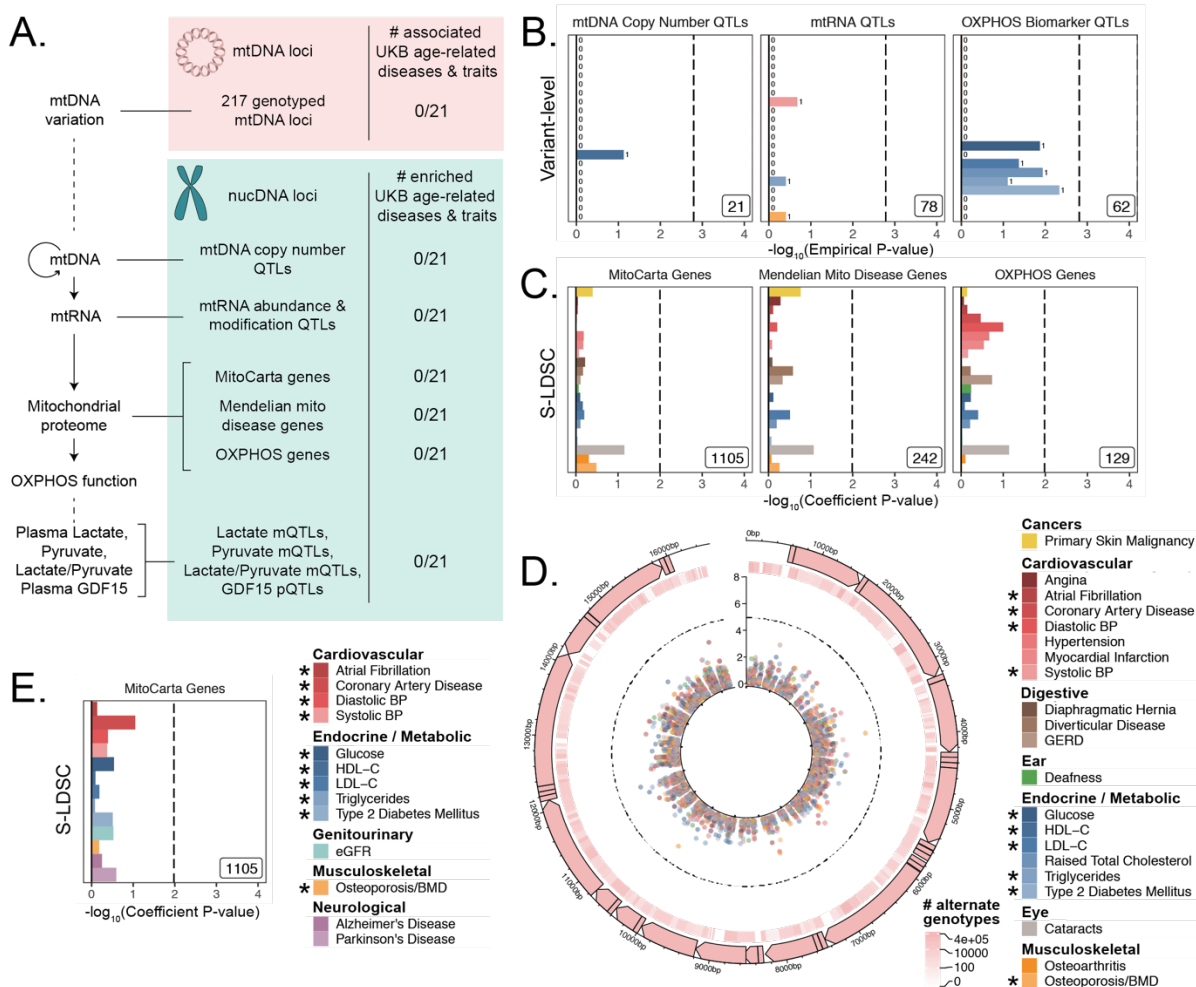


Figure 2. Assessment of the association of nucDNA and mtDNA mitochondria-relevant loci to age-related traits. **A.** Scheme outlining the aspects of mitochondrial function assessed in this study. nucDNA loci relevant to mitochondrial function are shown in teal, while mtDNA loci are shown in pink. **B.** Enrichment results for the overlap between loci associated with mtDNA copy number, mtRNA abundance/modification, and OXPHOS biomarkers and loci significantly associated with age-related disease in UKB. Inset number represents the number of tested SNPs, numbers adjacent to bars represent the absolute number of mitochondria-relevant loci overlapping the respective age-related disease. Dotted line represents Bonferroni cutoff for $p = 0.1$; BH FDR 0.1 threshold cannot be visualized as no tests pass the cutoff (**Supplementary note**). **C.** S-LDSC enrichment p-values on top of the baseline model in UKB. Inset labels represent gene-set size; dotted line represents BH FDR 0.1 threshold. **D.** Visualization of mtDNA variants and associations with age-related diseases. The outer-most track represents the genetic architecture of the circular mtDNA. The heatmap track represents the number of individuals with alternate genotype on log scale. The inner track represents mitochondrial genome-wide association p-values, with radial angle corresponding to position on the mtDNA and magnitude representing $-\log_{10}$ P-value. Dotted line represents Bonferroni cutoff for all tested trait-variant pairs. **E.** Replication of S-LDSC enrichment results in meta-analyses. Dotted line represents BH FDR 0.1 threshold. * represent traits for which sufficiently well powered cohorts from both UKB and meta-analyses were available. The trait color legend to the right of panel **D** applies to panels **B**, **C**, and **D**, representing UKB traits.

123 First, we tested if published QTLs for mtCN, mtRNA abundance, and OXPPOS biomarkers (**Table S3, S4**)
124 were enriched for an overlap with genome-wide significant loci for each of our age-related traits in UKB
125 (**Methods, Figure S2**). We observed no evidence of enrichment among QTLs available in the literature
126 (**Figure 2B, Supplementary note**; all $q > 0.1$).

127 Second, we used S-LDSC^{36,49} and MAGMA (<https://ctg.cncr.nl/software/magma>)⁵⁰, two robust methods
128 that can be used to assess gene-based heritability enrichment accounting for LD and several confounders,
129 to test if there was any evidence of heritability enrichment among MitoCarta genes (**Methods**). We found
130 no evidence of enrichment near nucDNA MitoCarta genes for any trait tested in UKB using S-LDSC (**Figure**
131 **2C, S8A**), consistent with our results from the GWAS Catalog. We replicated this lack of enrichment using
132 MAGMA at two different window sizes (**Figure S8C, S8E**; all $q > 0.1$).

133 Given the lack of enrichment among the MitoCarta genes, we wanted to (1) verify that our selected
134 methods could detect previously reported enrichments and (2) confirm that common variation in or near
135 MitoCarta genes can lead to expression-level perturbations. We first successfully replicated previously
136 reported enrichment among tissue-specific genes for key traits using both S-LDSC (**Figure S3, S4**) and
137 MAGMA (**Figure S5, S6, Supplementary note, Methods**). We next confirmed that we had sufficient power
138 using both S-LDSC and MAGMA to detect physiologically relevant enrichment effect sizes among
139 MitoCarta genes (**Figure S7, Methods, Supplementary note**). We finally examined the landscape of cis-
140 expression QTLs (eQTLs) for these genes and found that almost all MitoCarta genes have cis-eQTLs in at
141 least one tissue and often have cis-eQTLs in more tissues than most protein-coding genes (**Figure S9,**
142 **Methods, Supplementary note**). Hence, our selected methods could detect physiologically relevant
143 heritability enrichments among our selected traits at gene-set sizes comparable to that of MitoCarta, and
144 common variants in or near MitoCarta genes exerted *cis*-control on gene expression.

145 Third, we considered mtDNA loci genotyped in UKB, obtaining calls for up to 213 common variants passing
146 quality control across 360,662 individuals (**Methods, Supplementary note**). We found no significant
147 associations on the mtDNA for any of the 21 age-related traits available in UKB using linear or logistic
148 regression (**Methods, Figure 2E, S9**).

149 As a control and to validate our approach, we also performed mtDNA-GWAS for specific traits with
150 previously reported associations. A recent analysis of ~147,437 individuals in BioBank Japan revealed four
151 distinct traits with significant mtDNA associations⁵¹. Of these, creatinine and aspartate aminotransferase
152 (AST) had sufficiently large sample sizes in UKB. We observed a large number of associations throughout
153 the mtDNA for both traits ($p < 1.15 * 10^{-5}$, **Figure S9E**). Thus, our mtDNA association method was able to
154 replicate robust mtDNA associations among well-powered traits.

155 Finally, we sought to replicate our negative results in an independent cohort. We turned to published
156 GWAS meta-analyses²⁶⁻³⁵ (**Table S1**) and successfully replicated the lack of enrichment for MitoCarta
157 genes across all 10 traits with an available independent cohort GWAS using S-LDSC (**Figure 2E, S8B**) and
158 MAGMA at two different window sizes (**Figure S8D, Supplementary note**; all $q > 0.1$). Importantly, while
159 we were unable to pursue analyses for PD and Alzheimer's disease in UKB due to limited case counts, we
160 tested MitoCarta genes among well-powered meta-analyses for these disorders (**Supplementary note**)
161 and observed no enrichment (**Figure 2E**; all $q > 0.1$).

162 In summary, we tested (1) QTLs for mitochondrial physiology in UKB, (2) nucDNA loci near genes that
163 encode the mitochondrial proteome in the GWAS Catalog, UKB, and GWAS meta-analyses, (3) mtDNA
164 variants in UKB, and (4) known transcriptional regulators of mitochondrial biogenesis and function in the
165 GWAS Catalog. We found no convincing evidence of heritability enrichment for common age-associated
166 diseases among these mitochondria-relevant loci (**Table S8**).

167 **Enrichment of age-related trait heritability near genes encoding nuclear transcription factors**

168 We next asked whether heritability for age-related diseases and traits clusters among loci associated with
 169 any cellular organelle. We used the COMPARTMENTS database (<https://compartments.jensenlab.org>) to
 170 define gene-sets corresponding to the proteomes of nine additional organelles⁵² besides mitochondria
 171 (**Methods**). We used S-LDSC to produce heritability estimates for these categories in the UKB age-related
 172 disease traits, finding evidence of heritability enrichment in many traits for genes comprising the nuclear
 173 proteome (**Figure 3A, Methods**). No other tested organelles showed evidence of heritability enrichment.
 174 Variation in or near genes comprising the nuclear proteome explained over 50% of disease heritability on
 175 average despite representing only ~35% of tested SNPs (**Figure S10, Supplementary note**). We
 176 successfully replicated this pattern of heritability enrichment among organelles using MAGMA in UKB at
 177 two window sizes (**Figure S13A, S13B**), again finding only enrichment among genes related to the nucleus.
 178 With over 6,000 genes comprising the nuclear proteome, we considered largely disjoint subsets of the
 179 organelle's proteome to trace the source of the enrichment signal^{53–55} (**Figure 3B, Methods,**
 180 **Supplementary note**). We found significant heritability enrichment within the set of 1,804 genes whose
 181 protein products are annotated to localize to the chromosome itself ($q < 0.1$ for 9 traits, **Figure 3C, S12**).
 182 Further partitioning revealed that much of this signal is attributable to the subset classified as
 183 transcription factors⁵⁵ (1,523 genes, $q < 0.1$ for 10 traits, **Figure 3D, S12**). We replicated these results using
 184 MAGMA in UKB at two window sizes (**Figure S13**), and also replicated enrichments among TFs in several
 185 (but not all) corresponding meta-analyses (**Figure S14**) despite reduced power (**Figure S7H**). We generated
 186 functional subdivisions of the TFs (**Methods, Supplementary note**), finding that the non-zinc finger TFs

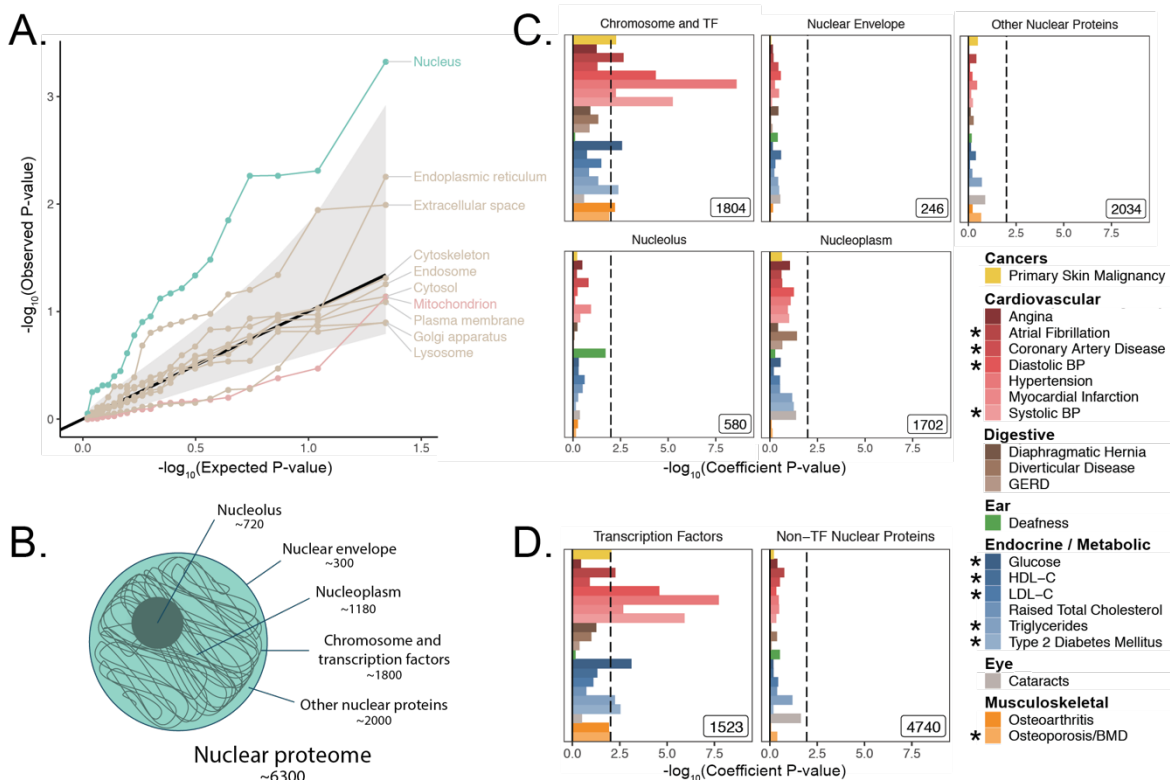


Figure 3. Heritability enrichment of organellar proteomes across age-related disease in UK Biobank. **A.** Quantile-quantile plot of heritability enrichment p-values atop the baseline model for gene-sets representing organellar proteomes, with black line representing expected null p-values following the uniform distribution and shaded ribbon representing 95% CI. **B.** Scheme of spatially disjoint subsets of the nuclear proteome as a strategy to characterize observed enrichment of the nuclear proteome. Numbers represent gene-set size. **C.** S-LDSC enrichment p-values for spatial subsets of the nuclear proteome computed atop the baseline model. **D.** S-LDSC enrichment p-values for TFs and all other nucleus-localizing proteins. Inset numbers represent gene-set sizes, black lines represent cutoff at BH FDR < 10%. * represent traits for which sufficiently well powered cohorts from both UKB and meta-analyses were available.

187 showed enrichment for a highly similar set of traits to those enriched for the whole set of TFs (**Figure**
 188 **S15D, S16B, S17B, S18B**). Interestingly, the KRAB domain-containing zinc fingers (KRAB ZFs)⁵⁶, which are
 189 recently evolved (**Figure S15H**), were largely devoid of enrichment even compared to non-KRAB ZFs
 190 (**Figure S15E, S16C, S17C, S18C**). Thus, we find that variation within or near non-KRAB domain-containing
 191 transcription factor genes has an outsize influence on age-associated disease heritability (**Table S8**).

192

193 **Mitochondrial genes tend to be more “haplosufficient” than genes encoding other organelles**

194 In light of observing heritability enrichment only among nuclear transcription factors, we wanted to
 195 determine if the fitness cost of pLoF variation in genes across cellular organelles mirrored our results.
 196 Mitochondria-localizing genes and TFs play a central role in numerous Mendelian diseases^{19,57–59}, so we
 197 initially hypothesized that genes belonging to either category would be under significant purifying
 198 selection (i.e., constraint). We obtained constraint metrics from gnomAD

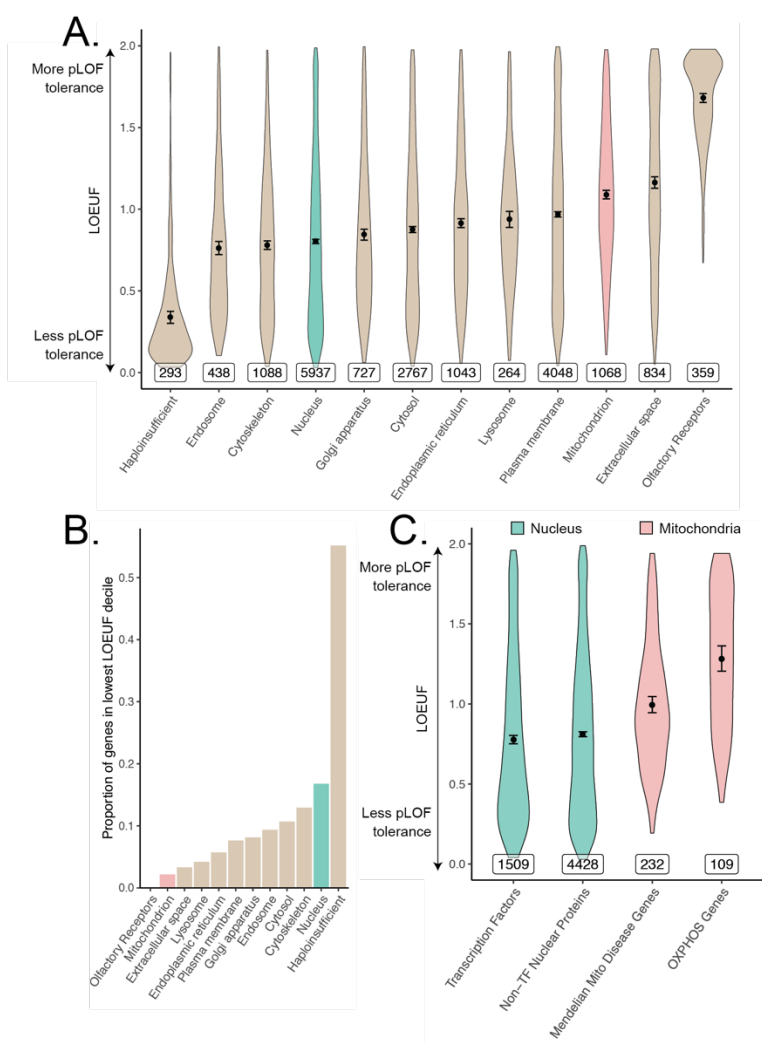


Figure 4. Differences in constraint distribution across organelles. **A.** Constraint as measured by LOEUF from gnomAD v2.1.1 for genes comprising organellar proteomes, book-ended by distributions for known haploinsufficient genes as well as olfactory receptors. Lower values indicate genes exacting a greater organismal fitness cost from a heterozygous LoF variant (greater constraint). **B.** Proportion of each gene-set found in the lowest LOEUF decile. Higher values indicate gene-sets containing more highly constrained genes. **C.** Constraint distributions for subsets of the nuclear-encoded mitochondrial proteome (red) and subsets of the nucleus (teal). Black points represent the mean with 95% CI. Inset numbers represent gene-set size.

199 (<https://gnomad.broadinstitute.org>)⁶⁰ as the LoF observed/expected fraction (LOEUF). In agreement with
200 our GWAS enrichment results, we observed that the mitochondrion on average is one of the least
201 constrained organelles we tested, in stark contrast to the nucleus (**Figure 4A**). In fact, the nucleus was
202 second only to the set of “haploinsufficient” genes (defined based on curated human clinical genetic
203 data⁶⁰, **Methods**) in the proportion of its genes in the most constrained decile, while the mitochondrion
204 lay on the opposite end of the spectrum (**Figure 4B**). Interestingly, even the Mendelian mitochondrial
205 disease genes had a high tolerance to pLoF variation on average in comparison to TFs (**Figure 4C, S19A**).
206 Even across different categories of TFs, we observed that highly constrained TF subsets tend to show
207 GWAS enrichment (**Figure S19B, S15E**) relative to unconstrained subsets for our tested traits. Indeed,
208 explicit inclusion of LOEUF as a covariate in the enrichment analysis model (**Methods**) reduced the
209 significance of (but did not eliminate) the enrichment seen for the TFs (**Figure S20B, S21B, S20E, S20F**).
210 Thus, while disruption in both mitochondrial genes and TFs can produce rare disease, the fitness cost of
211 heterozygous variation in mitochondrial genes appears to be far lower than that among the TFs. This
212 dichotomy reflects the contrasting enrichment results between the mitochondrial genes and the TFs and
213 supports the importance of gene regulation as it relates to evolutionary conservation.

214

215 **Discussion**

216 Organelle pathology has been documented in many age-related diseases^{3,23,61–64}. Perhaps most notably, a
217 decline in mitochondrial abundance and activity has long been reported as one of the most consistent
218 biomarkers of aging^{4,9,14,15} and of heritable age-associated diseases such as T2D^{5,6,10–12}, PD^{8,13}, and CVD^{7,16}.
219 This suggested that variation in loci relevant to mitochondrial function may explain a disproportionate
220 amount of heritability for these age-related traits. We tested mitochondria-relevant common variants on
221 the nucDNA and mtDNA in the GWAS Catalog, UKB, and meta-analyses using Fisher’s exact tests, S-LDSC,
222 and MAGMA. We found no convincing evidence of heritability enrichment among mitochondria-relevant
223 loci in any tested trait, cohort, or method. Of 10 tested organelles, only the nucleus showed enrichment,
224 and further analysis revealed that much of this signal originated from transcription factors. These
225 contrasting results were corroborated by constraint analysis, which showed a substantial fitness cost to
226 heterozygous loss-of-function mutation in genes encoding the nuclear proteome, whereas genes
227 encoding the mitochondrial proteome were “haplosufficient.”

228 For highly polygenic and well-powered traits, any large fraction of the genome may explain a statistically
229 significant amount of disease heritability^{65,66}. Indeed, individual associations between mitochondria-
230 relevant loci and certain common diseases have been identified previously^{67,68}. As associations have also
231 been identified among loci relevant for other organelles, enrichment analyses can place these complex
232 genetic architectures in a broader biological context and prioritize pathways for follow-up. Importantly,
233 both MAGMA and S-LDSC are capable of detecting an enrichment even in a highly polygenic background.
234 Both methods have been used in the past to identify biologically plausible disease-relevant tissues^{36,49} and
235 pathway enrichments^{69,70} in traits across the spectrum of polygenicity, and we identify enrichments
236 among disease-relevant tissues using both methods in several highly polygenic traits.

237 Our comprehensive analysis of common inherited mitochondrial variation is in agreement with the
238 literature and represents, to our knowledge, the most comprehensive assessment of such variation in
239 age-related diseases to date. Our negative results are consistent with a small number of isolated reports
240 interrogating either mitochondria-relevant nucDNA⁷¹ or mtDNA^{51,72–74} loci in cardiometabolic traits,
241 cataracts, osteoporosis, or osteoarthritis. We replicated mtDNA associations with creatinine and AST
242 observed previously in BioBank Japan⁵¹, further supporting our approach. While individual mtDNA
243 variants have been previously associated with certain traits^{75–77}, these associations appear to be
244 conflicting in the literature, perhaps because of limited power and/or uncontrolled confounding biases
245 such as population stratification^{78,79}.

246 Though several organelles have been associated with aging and age-associated pathology^{3,23,61–64}, of the
247 ten organelles we considered, we observed age-related trait heritability enrichment for only one: the
248 nucleus. While previous work has shown that common disease GWAS can be enriched for expression in
249 specific disease-relevant organs^{49,80}, this framework does not appear to extend to organelles outside the
250 nucleus. This finding contrasts with our classical nosology of (typically recessive) inborn errors of
251 metabolism that tend to be mapped to “causal” organelles, e.g., lysosomal storage diseases, disorders of
252 peroxisomal biogenesis, and mitochondrial OXPHOS disorders. The enrichment of the nucleus appears to
253 derive almost entirely from transcription factors, indicating that common variation influencing genome
254 regulation impacts the inherited risk of common diseases more than variation influencing individual
255 organelles.

256 Our observation that MitoCarta genes are pLoF tolerant (**Figure 4A**) is consistent with the rare disease
257 literature. Namely, while mutations in over 300 nucDNA genes can produce severe Mendelian
258 mitochondrial disease¹⁹, the vast majority tend to be autosomal recessive with healthy parents. The few
259 disorders that show dominant inheritance are nearly always due to dominant negativity rather than
260 haploinsufficiency. In combination with these observations, the results from the current study indicate
261 that mitochondrial pathways are generally haplosufficient.

262 The observed pLoF-intolerance among TFs (**Figure 4A**) provide a stark contrast to the results from the
263 mitochondria that is borne out in their associated Mendelian disease syndromes: TFs are known to be
264 haploinsufficient⁸¹ and even regulatory variants modulating their expression can produce severe
265 Mendelian disease⁸². We observe heritability enrichment among TFs for 10 different diseases, consistent
266 with observed elevated purifying selection against pLoF variants in these genes. Our enrichment results
267 combined with pLoF intolerance suggest that variation among TFs may produce disease-associated
268 variants with larger effect sizes than expectation. Overall, gene-regulatory pathways at the level of the
269 TFs appear to be less resilient to common variation and more susceptible to conferring disease risk upon
270 genetic perturbation. These results highlight the importance of gene regulators and suggest that they may
271 serve as important genetic “levers” for the modulation of pathways relevant to common disease
272 heritability.

273 Why are mitochondria so robust to variation in gene dosage and hence haplosufficient? We propose three
274 possibilities. First, pathway redundancy may underlie robustness to mitochondrial insults, consistent with
275 the longstanding observation that in cell culture, defective OXPHOS can be supported thanks to the action
276 of non-mitochondrial pathways such as cytosolic glycolysis and nucleotide salvage as long as key
277 environmental nutrients are provided⁸³. Second, mitochondrial pathways tend to be highly
278 interconnected, and it was already proposed by Wright⁸⁴ and later by Kacser and Burns⁸⁵ that
279 haploinsufficiency arises as a consequence of physiology, i.e., network organization of metabolic reactions.
280 Kacser and Burns in fact explicitly mention that noncatalytic gene products fall outside their framework,
281 and we believe that our finding that nucleus-localizing and cytoskeletal genes are the two most pLoF-
282 intolerant compartments is consistent with their assessment. Third, mitochondria were formerly
283 autonomous microbes and hence may have retained vestigial layers of “intra-organelle buffering” against
284 genetic variation. Numerous feedback control mechanisms, including respiratory control⁸⁶, help to ensure
285 organelle robustness across physiological extremes⁸⁷ (e.g. resting versus exercising⁸⁸, shifting nutrient
286 availability). In agreement, a recent CRISPR screen showed that of the genes for which knock-out modified
287 survival under a mitochondrial poison, there is a striking over-representation of genes that themselves
288 encode mitochondrial proteins⁸⁹.

289 Throughout this study, we have tested inherited common variant associations via an additive genetic
290 model. We acknowledge the limitations of focusing on a specific genetic model and variant frequency
291 regime, though note that common variation is the largest documented source of narrow-sense

292 heritability, which typically accounts for a majority of disease heritability^{90,91}. First, we consider only
293 common variants. While rare variants may prove to be instructive, it is notable that a previous rare variant
294 analysis in T2D⁹² failed to show enrichment among OXPHOS genes. Second, we consider only additive
295 genetic models. A recessive model may be particularly fruitful for mitochondria-relevant loci given their
296 tolerance to pLoF variation, however these models are frequently power-limited and may not explain
297 much more phenotypic variance than additive models^{93,94}. Third, we have not considered epistasis. The
298 effects of mtDNA-nucDNA interactions⁹⁵ in common diseases have yet to be assessed. While there is
299 debate about whether biologically-relevant epistasis can be simply captured by main effects^{91,93,96,97} at
300 individual loci, it is possible that modeling mtDNA-nucDNA interactions will reveal new contributions.
301 Finally, it is crucial not to confuse our results with previously reported associations between somatic
302 mtDNA mutations and age-associated disease¹³⁻¹⁵ – the present work is focused on germline variation.

303 Our study does not formally address the causality of mitochondrial dysfunction in common age-related
304 disease. Rather, we have tested if common variants in mitochondrial pathways tend to explain a
305 disproportionate amount of age-related disease heritability. The observed lack of heritability enrichment
306 in mitochondrial pathways does not preclude the possibility of a therapeutic benefit in targeting the
307 mitochondrion for age-related disease. For example, mitochondrial dysfunction is documented in brain or
308 heart infarcts following blood vessel occlusion in laboratory-based models^{98,99}. Though mitochondrial
309 variants do not influence infarct risk in this laboratory model, pharmacological blockade of the
310 mitochondrial permeability transition pore can mitigate reperfusion injury and infarct size¹⁰⁰. Future
311 studies will be required to determine if and how the mitochondrial dysfunction associated with common
312 age-associated diseases can be targeted for therapeutic benefit.

313 Our finding that the nucleus is the only organelle that shows enrichment for common age-associated trait
314 heritability builds on prior work implicating nuclear processes in aging. Most human progeroid syndromes
315 result from monogenic defects in nuclear components¹⁰¹ (e.g., *LMNA* in Hutchinson-Gilford progeria
316 syndrome, *TERC* in dyskeratosis congenita), and telomere length has long been observed as a marker of
317 aging¹⁰². Heritability enrichment of age-related traits among gene regulators is consistent with the
318 epigenetic dysregulation¹⁰³ and elevated transcriptional noise^{3,104} observed in aging (e.g., *SIRT6*
319 modulation influences mouse longevity¹⁰⁵ and metabolic syndrome⁶²). An important role for gene
320 regulation in common age-related disease is in agreement with both the observation that a very large
321 fraction of common disease-associated loci corresponds to the non-coding genome and the enrichment
322 of disease heritability in histone marks and transcription factor binding sites^{36,106}.

323

324 **Acknowledgements**

325 We thank D. Altshuler, S.E. Calvo, H. Finucane, E.S. Lander, M.E. MacDonald, D. Palmer, E.B. Robinson,
326 A.V. Segrè, M.E. Talkowski, R.K. Walters, C.C. Winter, and members of the Mootha and Neale labs for
327 critical feedback and discussions. This research has been conducted using the UK Biobank Resource under
328 Application Number 31063. This project was supported in part by grants (NIH R35GM122455 to V.K.M.
329 and NIH T32 AG000222 to R.G.) from the National Institutes of Health. VKM is an Investigator of the
330 Howard Hughes Medical Institute.

331

332 **Data Availability**

333 Genetic correlation point estimates and standard errors plotted in Figure 1B is available in Table S2.
334 Summary statistics from mtDNA-GWAS available in Table S6. All gene-based enrichment analysis p-values
335 and point estimates are available in Table S8. Literature-reported loci associated with biomarkers of
336 mitochondrial function after clumping and QC are available in Table S4. Period prevalence data for
337 diseases in the UK can be obtained from Kuan et al. 2019. Gene-sets can be found using COMPARTMENTS

338 (<https://compartments.jensenlab.org>), MitoCarta 2.0
339 (<https://www.broadinstitute.org/files/shared/metabolism/mitocarta/human.mitocarta2.0.html>),
340 Lambert et al. 2018 (DOI: 10.1016/j.cell.2018.01.029), Frazier et al. 2019 (DOI: 10.1074/jbc.R117.809194),
341 Finucane et al. 2018 (<https://alkesgroup.broadinstitute.org/LDSCORE/>), Kapopoulou et al. 2015 (DOI:
342 10.1111/evo.12819), and the Macarthur laboratory (https://github.com/macarthur-lab/gene_lists). Gene
343 age estimates were obtained from Litman, Stein 2019 (DOI: 10.1053/j.seminoncol.2018.11.002). GWAS
344 catalog annotations can be obtained from: <https://www.ebi.ac.uk/gwas>. UKB heritability estimates can
345 be obtained at: https://nealelab.github.io/UKBB_ldsc/. UKB summary statistics can be obtained from
346 Neale lab GWAS round 2: https://github.com/Nealelab/UK_Biobank_GWAS. Annotations for the Baseline
347 v1.1 and BaselineLD v2.2 models as well as other relevant reference data, including the 1000G EUR
348 reference panel, can be obtained from <https://alkesgroup.broadinstitute.org/LDSCORE/>. eQTL and
349 expression data in human tissues can be obtained from GTEx (<https://www.gtexportal.org>). Constraint
350 estimates can be found via gnomAD: <https://gnomad.broadinstitute.org>. See citations for publicly
351 available GWAS meta-analysis summary statistics^{26–35}.

352

353 **Code Availability**

354 Our analysis leverages publicly available tools including LDSC for heritability enrichment and genetic
355 correlation (<https://github.com/bulik/ldsc>), MAGMA v1.07b for gene-set enrichment analysis
356 (<https://ctg.cncr.nl/software/magma>), PLINK v1.07 for linkage disequilibrium clumping
357 (<https://zzz.bwh.harvard.edu/plink/>), and Hail v0.2.51 for distributed computing and mtDNA GWAS
358 (<https://hail.is>).

359

360 **Competing Interests**

361 VKM is an advisor to and receives compensation or equity from Janssen Pharmaceuticals, 5am Ventures,
362 and Raze Therapeutics. BMN is a member of the scientific advisory board at Deep Genomics and RBNC
363 Therapeutics. BMN is a consultant for Camp4 Therapeutics, Takeda Pharmaceutical and Biogen.

364

365 **Author Contributions**

366 R.G., B.M.N., and V.K.M. conceived of the project; R.G., K.J.K., D.H. designed analyses; R.G. performed
367 analyses; B.M.N., V.K.M. supervised project; R.G. and V.K.M. wrote the manuscript with input from
368 other authors.

369 **Online Methods**

370 Trait selection:

371 Sex-standardized period prevalence of over 300 diseases was obtained from an extensive survey of the
372 National Health Service in the UK as reported previously²⁴. To select high prevalence late-onset diseases,
373 we ranked diseases with a median onset over 50 years of age by the sum of the period prevalence of all
374 age categories above 50. We selected the top 30 diseases using this metric and manually mapped these
375 traits to similar or equivalent phenotypes with publicly available summary statistics from UKB and/or well-
376 powered meta-analyses (e.g., Parkinson's Disease and Alzheimer's Disease for dementia) resulting in 24
377 traits with data available in UKB, meta-analyses, or both (**Table S1**).

378

379 Criteria for inclusion of summary statistics:

380 We manually mapped selected age-related diseases and traits to corresponding phenotypes in UKB. In
381 parallel, we searched the literature to identify well-powered EUR-predominant GWAS (referred to as
382 meta-analyses) that (1) used primarily non-targeted arrays, (2) had publicly available full summary
383 statistics, and (3) did not enroll individuals from UKB to serve as independent replication (**Supplementary**
384 **note**). For UKB, we obtained heritability estimates (https://github.com/Nealelab/UKBB_ldsc) previously
385 computed using stratified linkage-disequilibrium score regression (S-LDSC,
386 <https://github.com/bulik/ldsc>)³⁶ atop the BaselineLD v1.1 model using reference LD scores computed
387 from 1000G EUR. For meta-analyses, we computed heritability estimates with S-LDSC atop the updated
388 BaselineLD v2.2 model using reference LD scores computed from 1000G EUR
389 (<https://alkesgroup.broadinstitute.org/LDSCORE/>). We computed the heritability Z-score, a statistic that
390 captures sample size, polygenicity, and heritability³⁶, and included only traits with heritability Z-score > 4
391 (**Supplementary note**) for further analysis.

392

393 Genetic correlations in UKB:

394 Pairwise genetic correlations, r_g , were computed using linkage-disequilibrium score correlation³⁷ on all
395 selected age-related traits with heritability Z-score > 4. We used UKB summary statistics
396 (https://github.com/Nealelab/UK_Biobank_GWAS) for all sufficiently powered traits; summary statistics
397 from meta-analyses were used for eGFR³³, Alzheimer's Disease³⁵, and Parkinson's Disease³⁴ as these traits
398 showed heritability Z-score > 4 within meta-analyses but not in UKB (**Table S1**). P-values for genetic
399 correlation represented deviation from the null hypothesis $r_g = 0$. Traits were ordered by their
400 contribution to the first eigenvector of the absolute value of the correlation matrix, with point estimates
401 and standard errors available in **Table S2**. Bonferroni correction was applied producing a p-value cutoff of
402 $0.05/\binom{24}{2} = 1.81 * 10^{-4}$.

403

404 Assessment of mitochondria-localizing genes in the GWAS Catalog:

405 We mapped variants in the GWAS Catalog (obtained on September 5th, 2019,
406 <https://www.ebi.ac.uk/gwas/>) meeting genome-wide significance ($p < 5e-8$) to genes using provided
407 annotations, producing a set of trait-associated genes for each trait. We manually selected phenotypes
408 represented in the GWAS Catalog matching our set of age-associated traits with over annotated 30 trait-
409 associated genes. For each trait, we computed the proportion of trait associated genes that were
410 mitochondria-localizing (defined via MitoCarta2.0¹⁷) and tested for enrichment or depletion relative to
411 overall genome background using two-sided Fisher's exact tests correcting for multiple hypothesis tests
412 with the Benjamini-Hochberg (BH) procedure at FDR q-value < 0.1.

413 We also computed the test statistic N_g^{enrich} , defined as the number of age-associated traits showing a
414 nominal (not necessarily statistically significant) enrichment for a given gene-set g , for the MitoCarta
415 genes. We then generated an empirical null distribution for N_g^{enrich} . We drew 1,000 random samples of

416 protein-coding genes, where each sample contained the same number of genes as the set of
417 mitochondria-localizing genes and computed N_g^{enrich} for each of these gene-sets (**Figure S1B**). The one-
418 sided p-value, defined as $\Pr(N_g^{enrich} \leq x)$ under the null, was subsequently obtained.

419 We expanded our enrichment/depletion analysis to all 332 traits in the GWAS Catalog with over 30 trait-
420 associated genes; for enrichment or depletion testing, we used two-sided Fisher's exact tests and
421 corrected for multiple hypothesis testing with the BH procedure at FDR q-value < 0.1.

422 Enrichment analysis of literature-curated mitochondria-associated phenotypes:

423 We reviewed the literature for quantitative trait loci (QTLs) for mtDNA copy number (mtCN)^{40,41}, mtRNA
424 abundance/modification^{42,43}, and biomarkers of OXPHOS dysfunction (namely lactate, pyruvate,
425 lactate/pyruvate ratio⁴⁶⁻⁴⁸, and GDF15 abundance^{44,45}) (**Supplementary note**). We subsequently used
426 PLINK v1.07 (<https://zzz.bwh.harvard.edu/plink/>)¹⁰⁷ to identify independent variants for each phenotype
427 based on the 1000G EUR reference panel (**Supplementary note**). To test for overlap with UKB age-
428 associated disease traits, we divided curated variants into three classes: mtCN-related (21 variants),
429 mtRNA-related (78 variants), and OXPHOS biomarkers (62 variants). For each of the 21 UKB age-related
430 disease traits, we computed the number of genome-wide significant ($p < 5e-8$) variants that overlapped
431 the curated variants for each class, termed $N_c^{overlap}$ where c is the class. We only considered variants
432 with INFO > 0.8 and MAF > 0.001 or expected case MAC > 25. For significance testing, we generated an
433 empirical null distribution around $N_c^{overlap}$ including only variants with INFO > 0.8. For each class, we
434 drew variants at random 2500 times matching on LD score, in-sample MAF, and distance to transcription
435 start site (where the distance metric was set to 0 if the variant was located within a gene boundary). LD
436 scores per variant were generated per-chromosome with a 1 cm window using the 1000G EUR reference
437 panel. The $N_c^{overlap}$ was then computed for each category for each set of randomly selected variants,
438 generating a category specific empirical null distribution for the statistic (**Figure S2**). The one-sided p-
439 value, defined as $\Pr(N_c^{overlap} \geq x)$ under the null, was subsequently obtained. To correct for multiple
440 hypothesis testing, we applied the BH procedure with FDR < 0.1 and also applied a Bonferroni threshold
441 of $P = \frac{0.1}{21*3} \approx 0.0016$.

442 Harmonization and filtering of summary statistics for LDSC and MAGMA:

443 UKB summary statistics previously formatted for use with LDSC and filtered to HapMap3 (HM3) SNPs
444 (https://github.com/Nealelab/UKBB_ldsc) were used for analysis with S-LDSC. For analysis with MAGMA
445 v1.07b⁵⁰, we included variants from the full Neale Lab UKB Round 2 GWAS summary statistics
446 (https://github.com/Nealelab/UK_Biobank_GWAS) with INFO > 0.8 and MAF > 0.01, and excluded any
447 variants flagged as low confidence (a heuristic defined by MAF < 0.001 or expected case MAC < 25).

448 Summary statistics obtained from publicly available GWAS meta-analyses²⁶⁻³⁵ were reported in varied
449 formats. We manually verified the genome build upon which each meta-analysis reported results and
450 ensured that all sets of summary statistics contained columns listing P-value, variant rsID, genome-build
451 specific coordinates, and if available, variant-specific sample size (**Table S1**). If variant coordinates or rsID
452 were not provided, the relevant columns were obtained from dbSNP database version 130 (for hg18) or
453 146 (for hg19). We used the summary statistic munging script provided with S-LDSC
454 (<https://github.com/bulik/ldsc>) to generate summary statistics compatible with S-LDSC, restricting to
455 HM3 SNPs as these tend to be best behaved for analysis with LDSC. For use of meta-analyses with
456 MAGMA⁵⁰, we restricted analysis to variants with INFO > 0.8 and MAF > 0.01 if such information was
457 provided.

458 Multiple testing correction for gene-set enrichment analysis:

462 To account for the multiple hypothesis tests performed throughout this study, we obtained p-value
463 thresholds via the BH procedure at FDR < 0.1 for all gene-sets assessed for a given method and cohort
464 type (where the two cohort types were UKB and meta-analysis).

465

466 *Gene-set based enrichment analysis:*

467 We extensively use S-LDSC and MAGMA to perform gene-set enrichment analyses among GWAS summary
468 statistics. To test enrichment with S-LDSC, SNPs were mapped to each gene with a 100kb symmetric
469 window as recommended⁴⁹ and LD scores were computed using the 1000G EUR reference panel
470 (<https://alkesgroup.broadinstitute.org/LDSCORE/>) and subsequently restricted to the HM3 SNPs. We
471 used S-LDSC to test for heritability enrichment controlling for 53 annotations including coding regions,
472 enhancer regions, 5' and 3' UTRs, and others as previously described³⁶ (baseline v1.1, referred to as
473 baseline model hereafter). We also used MAGMA with both 5kb up, 1.5kb down and 100kb symmetric
474 windows to test for enrichment. MAGMA gene-level analysis was performed with the 1000G EUR LD
475 reference panel to account for LD structure, and gene-set analysis was performed including covariates for
476 gene length, variant density, inverse minor allele count (MAC), as well as log-transformed versions of
477 these covariates. Statistical tests for both S-LDSC and MAGMA were one-sided, considering enrichment
478 only. For both methods, we included the relevant superset of genes as a control to ensure that our analysis
479 was competitive (**Supplementary note**). We refer to this approach as the 'usual approach'. All enrichment
480 effect size estimates and p-values are available in **Table S8**.

481

482 *Enrichment analysis of genes comprising the mitochondrial proteome:*

483 We obtained the set of nuclear-encoded mitochondria-localizing genes using MitoCarta2.0¹⁷ and used the
484 literature to obtain the subset of MitoCarta genes involved in inherited mitochondrial disease¹⁹ as well as
485 those producing components of oxidative phosphorylation (OXPHOS) complexes. We used both S-LDSC
486 and MAGMA to test for enrichment in the usual way (**Methods**) controlling for the set of protein-coding
487 genes to ensure a competitive analysis (**Supplementary note**). We also tested mitochondria-localizing
488 genes for enrichment in meta-analyses using S-LDSC and MAGMA with the same parameters as for UKB
489 traits (**Supplementary note**).

490

491 *Tissue-expressed gene-set enrichment analysis:*

492 To obtain the set of genes most expressed in a given tissue versus others, we obtained t-statistics
493 computed from GTEx v6 gene-level transcript-per-million (TPM) data corrected for age and sex as
494 published previously⁴⁹. For each tissue, we selected the top 2485 genes (10%) with the highest t-statistics
495 for tissue-specific expression, producing tissue-expressed gene-sets. We selected nine tissues based on
496 expectation of enrichment for our tested traits in UKB (e.g., liver for LDL levels, esophageal mucosa for
497 GERD). We used both S-LDSC and MAGMA to test for enrichment in the usual way (**Methods**) controlling
498 for the set of tissue-expressed genes to ensure a competitive analysis (**Supplementary note**). Tissue-
499 expressed gene-set analyses were performed on meta-analyses with S-LDSC and MAGMA on the same
500 tissues using the same parameters as used in UKB.

501

502 *Power analysis:*

503 To test for the effects of gene-set size on power, we selected ten positive control tissue-trait pairs based
504 on (1) the presence of tissue enrichment in UKB with S-LDSC and MAGMA and (2) if the observed
505 enrichment was biologically plausible. The pairs tested were liver-HDL, liver-LDL, liver-TG, liver-
506 cholesterol, pancreas-glucose, pancreas-type 2 diabetes, atrial appendage-atrial fibrillation, sigmoid
507 colon-diverticular disease, coronary artery-myocardial infarction, and visceral adipose-HDL. We then, in
508 brief, used an empirical sampling-based approach, generating random subsamples of a selected set of
509 tissue-expressed gene-sets at four different gene-set sizes (1523, 1105, 800, and 350 genes), defining

510 power as the proportion of trials showing a significant enrichment (**Supplementary note**). We used the
511 same sub-sampled gene-sets for enrichment analysis using both S-LDSC and MAGMA in the usual way
512 (**Methods**) controlling for the set of tissue-expressed genes to ensure a competitive analysis
513 (**Supplementary note**). We used the same gene-sets among the subset of the positive control traits that
514 showed enrichment in the corresponding meta-analysis to verify power for the meta-analyses
515 (**Supplementary note**).

516

517 Cross-tissue eQTL analysis

518 We obtained the set of eGenes from GTEx v8 across 49 tissues (<https://www.gtexportal.org>), filtering to
519 only include cis-eQTLs with q-value < 0.05. To determine how the landscape of cis-eQTLs for MitoCarta
520 genes compared to other protein-coding genes, we regressed the number of tissues with a detected cis-
521 eQTL for a given gene x , N_x^{eQTL} , onto an indicator for membership in a given organellar proteome
522 ($I_x^{organelle}$), controlling for gene length, log gene length, breadth of expression (τ_x), and the number of
523 tissues with detected expression > 5 TPM ($N_x^{express}$, **Supplementary note**). To quantify breadth of
524 expression, we obtained median-per-tissue GTEx v8 TPM expression values and computed τ^{108} after
525 removing lowly-expressed genes with maximal cross-tissue TPM < 1, defined as:

526

$$527 \tau_x = \frac{\sum_{i=1}^n (1 - \hat{x}_i)}{n - 1} \text{ where } \hat{x}_i = \frac{x_i}{\max_{1 \leq i \leq n} x_i}$$

528

529 where x_i is the expression of gene x in tissue i with n tissues. τ ranges from 0 to 1, with lower τ indicating
530 broadly expressed gene and higher τ indicating more tissue specific expression patterns. Because GTEx
531 sampled multiple tissue subtypes (e.g., brain sub-regions) that show correlated expression profiles¹⁰⁹
532 which bias τ_x , N_x^{eQTL} , and $N_x^{express}$ upward, for each broader tissue class (brain, heart, artery, esophagus,
533 skin, cervix, colon, adipose) we selected a single representative tissue when computing these quantities
534 (**Figure S14B, Supplementary note**). We used LD scores computed from the 1000G EUR reference panel.
535 The model, fit via OLS for each tested organelle, was:

536

$$537 N_x^{eQTL} \sim I_x^{organelle} + N_x^{express} + \tau_x + \log(\text{gene length}) + \text{gene length}$$

538

539 mtDNA-wide association study:

540 We obtained mtDNA genotype data on 265 variants as obtained on the UK Biobank Axiom array and the
541 UK BiLEVE array from the full UKB release²⁵. To perform variant QC, we used evoker-lite¹¹⁰ to generate
542 fluorescence cluster plots per-variant and per-batch and manually inspected the results, removing 19
543 variants due to cluster plot abnormalities (**Table S5, Supplementary note**). We additionally removed any
544 variants with heterozygous calls, within-array-type call rate < 0.95, and with less than 20 individuals with
545 an alternate genotype. For case-control traits, we removed any phenotype-variant pair with an expected
546 case count of alternate genotype individuals of less than 20, resulting in a maximum of 213 variants tested
547 per trait (**Supplementary note**). To perform sample QC, we restricted samples to the same samples from
548 which UKB summary statistics were generated (https://github.com/Nealelab/UK_Biobank_GWAS),
549 namely unrelated individuals 7 standard deviations away from the first 6 European sample selection PCs
550 with self-reported white-British, Irish, or White ethnicity and no evidence of sex chromosome aneuploidy.
551 We additionally removed any samples with within-array-type mitochondrial variant call rate < 0.95,
552 resulting in 360,662 unrelated samples of EUR ancestry. We generated the LD matrix for mitochondrial
553 DNA variants using Hail v0.2.51 (<https://hail.is>) pairwise for all 213 variants tested across all post-QC
554 samples.

555 We ran mtDNA-GWAS for all 21 UKB age-related phenotypes as well as creatinine and AST using Hail
556 v0.2.51 via linear regression controlling for the first 20 PCs of the nuclear genotype matrix, sex, age, age²,
557 sex*age, and sex*age² as performed for the UKB GWAS
558 (https://github.com/Nealelab/UK_Biobank_GWAS). We also used Hail to run Firth logistic regression with
559 the same covariates for case/control traits (**Table S1**). As we observed that some mitochondrial DNA
560 variants were specific to array type, we also ran linear regression including array type as a covariate; we
561 did not perform logistic regression with array type as a covariate due to convergence issues secondary to
562 complete separation of variants assessed only on only array type. We defined mtDNA-wide significance
563 using a Bonferroni correction by $p = \frac{0.05}{4337} \approx 1.15e - 5$.

564

565 *Enrichment analysis of components of organelle proteomes:*

566 COMPARTMENTS (<https://compartments.jensenlab.org>)⁵² is a resource integrating several lines of
567 evidence for protein localization predictions including annotations, text-mining, sequence predictions,
568 and experimental data from the Human Protein Atlas. We used this resource to obtain the degree of
569 evidence (a number ranging from 0 to 5) linking each gene to localization to one of 12 organelles: nucleus,
570 cytosol, cytoskeleton, peroxisome, lysosome, endoplasmic reticulum, Golgi apparatus, plasma
571 membrane, endosome, extracellular space, mitochondrion, and proteasome. To avoid noisy localization
572 assignments due to weak text mining and prediction evidence, we only considered localization
573 assignments with a score > 2 as described previously⁵². We subsequently assigned compartment(s) to each
574 gene by selecting the compartment(s) with the maximal score within each gene. We only included
575 compartments containing over 240 genes due to limited power at these smaller gene-set sizes and used
576 MitoCarta2.0¹⁷ to obtain a higher confidence set of genes localizing to the mitochondrion, resulting in
577 gene-sets representing the proteomes of 10 organelles. S-LDSC and MAGMA were used to test for
578 enrichment across the UKB age-related traits for these gene-sets in the usual way, controlling for the set
579 of protein-coding genes. S-LDSC was also used to obtain estimates of the percentage of heritability
580 explained by each organelle gene-set.

581

582 *Enrichment analysis of spatial components of the nucleus:*

583 To produce interpretable sub-divisions of the nucleus, we used Gene Ontology (GO)^{53,54} to identify terms
584 listed as children of the nucleus cellular component (GO:0005634). We used Ensembl version 99¹¹¹ to
585 obtain a first pass set of genes annotated to each sub-compartment of the nucleus (or its children). After
586 manual review of sub-compartments with > 90 genes, we selected nucleoplasm (GO:0005654), nuclear
587 chromosome (GO:0000228), nucleolus (GO:0005730), nuclear envelope (GO:0005635), splicosomal
588 complex (GO:0005681), nuclear DNA-directed RNA polymerase complex (GO:0055029), and nuclear pore
589 (GO:0005643). We excluded terms listed as 'part' due to poor interpretability and manually excluded
590 similar terms (e.g., nuclear lumen vs nucleoplasm). To generate a high confidence set of genes localizing
591 to each of these selected sub-compartments, we then turned to the COMPARTMENTS resource which
592 assigns localization confidence scores for each protein to GO cellular component terms. We assigned
593 members of the nuclear proteome to these selected nuclear sub-compartments using same the approach
594 outlined for the organelle analysis (**Methods**). After filtering our selected sub-compartments to those
595 containing > 240 genes, we obtained four categories: nucleoplasm, nuclear chromosome, nucleolus, and
596 nuclear envelope. The nuclear chromosome annotation was largely overlapping with a manually curated
597 high-quality list of transcription factors⁵⁵ however was not exhaustive; as such, we merged these lists to
598 generate the chromosome and TF category. To improve interpretability, we removed genes from
599 nucleoplasm that were also assigned to another nuclear sub-compartment, constructed a list of other
600 nucleus-localizing proteins not captured in these four sub-compartments, and included only genes
601 annotated as localizing to the nucleus (**Methods**). S-LDSC and MAGMA were used to test for enrichment

602 across the UKB age-related traits for these gene-sets in the usual way while controlling for the set of
603 protein-coding genes (**Methods**).

604

605 *Enrichment analysis of functionally distinct TF subsets:*

606 We used a published curated high-quality list of TFs⁵⁵ to partition the Chromosome and TF category into
607 transcription factors and other chromosomal proteins. To determine which TFs are broadly expressed
608 versus tissue specific, we computed τ per TF across all selected tissues after removing lowly-expressed
609 genes with maximal cross-tissue TPM < 1 (**Methods, Supplementary note**). The threshold for tissue-
610 specific genes was set at $\tau \geq 0.76$ based on the location of the central nadir of the resultant bimodal
611 distribution (**Figure S14A**). To identify terciles of TFs by age, we obtained relative gene age assignments
612 for each gene previously generated by obtaining the modal earliest ortholog level across several databases
613 mapped to 19 ordered phylostrata¹¹². DNA binding domain (DBD) annotations for the TFs were obtained
614 from previous manual curation efforts⁵⁵. S-LDSC and MAGMA were used to test for enrichment across the
615 UKB age-related traits for these gene-sets in the usual way while controlling for the set of protein-coding
616 genes (**Methods**). We also tested TFs for enrichment in meta-analyses using S-LDSC and MAGMA with the
617 same parameters as for UKB traits (**Supplementary note**).

618

619 *Analysis of constraint across organelles and sub-organelle gene-sets:*

620 We obtained gene-level gnomAD v2.1.1 constraint tables (<https://gnomad.broadinstitute.org>),
621 haploinsufficient genes, and olfactory receptors⁶⁰ (https://github.com/macarthur-lab/gene_lists).
622 Constraint values as loss-of-function observed/expected fraction (LOEUF) were mapped to genes within
623 organelle, sub-mitochondrial, sub-nuclear, and TF binding domain gene-sets.

624

625 *Enrichment analysis across age-related disease holding constraint as a covariate:*

626 To test for enrichment with constraint as a covariate, we used MAGMA with UKB age-related traits. We
627 mapped variants to genes and performed the gene-level analysis as done previously for the mitochondria-
628 localizing gene and organelle analysis. We included LOEUF and log LOEUF as covariates for the gene-set
629 analysis in addition to the default covariates (gene length, SNP density, inverse MAC, as well as the
630 respective log-transformed versions) via the `-condition-residualize` flag.

- 631 1. Wang K, Gaitsch H, Poon H, Cox NJ, Rzhetsky A. Classification of common human diseases derived
632 from shared genetic and environmental determinants. *Nat Genet.* 2017;49(9):1319-1325.
633 doi:10.1038/ng.3931
- 634 2. Claussnitzer M, Cho JH, Collins R, et al. A brief history of human disease genetics. *Nature.*
635 2020;577(7789):179-189. doi:10.1038/s41586-019-1879-7
- 636 3. López-Otín C, Blasco MA, Partridge L, Serrano M, Kroemer G. The hallmarks of aging. *Cell.*
637 2013;153(6):1194. doi:10.1016/j.cell.2013.05.039
- 638 4. Fleischman A, Makimura H, Stanley TL, et al. Skeletal muscle phosphocreatine recovery after
639 submaximal exercise in children and young and middle-aged adults. *J Clin Endocrinol Metab.*
640 2010;95(9):69-74. doi:10.1210/jc.2010-0527
- 641 5. Petersen KF, Dufour S, Befroy D, Garcia R, Shulman GI. Impaired Mitochondrial Activity in the
642 Insulin-Resistant Offspring of Patients with Type 2 Diabetes. *N Engl J Med.* 2004;350(7):664-671.
643 doi:10.1056/nejmoa031314
- 644 6. Mootha VK, Lindgren CM, Eriksson KF, et al. PGC-1 α -responsive genes involved in oxidative
645 phosphorylation are coordinately downregulated in human diabetes. *Nat Genet.* 2003;34(3):267-
646 273. doi:10.1038/ng1180
- 647 7. Fannin SW, Lesnefsky EJ, Slabe TJ, Hassan MO, Hoppel CL. Aging selectively decreases oxidative
648 capacity in rat heart interfibrillar mitochondria. *Arch Biochem Biophys.* 1999;372(2):399-407.
649 doi:10.1006/abbi.1999.1508
- 650 8. Schapira AH V, Cooper JM, Dexter D, Clark JB, Jenner P, Marsden CD. Mitochondrial Complex I
651 Deficiency in Parkinson's Disease. *J Neurochem.* 1990;54(3):823-827. doi:10.1111/j.1471-
652 4159.1990.tb02325.x
- 653 9. Trounce I, Byrne E, Marzuki S. Decline in Skeletal Muscle Mitochondrial Respiratory Chain
654 Function: Possible Factor in Ageing. *Lancet.* 1989;333(8639):637-639. doi:10.1016/S0140-
655 6736(89)92143-0
- 656 10. Kelley DE, He J, Menshikova E V., Ritov VB. Dysfunction of mitochondria in human skeletal muscle
657 in type 2 diabetes. *Diabetes.* 2002;51(10):2944-2950. doi:10.2337/diabetes.51.10.2944
- 658 11. Patti ME, Butte AJ, Crunkhorn S, et al. Coordinated reduction of genes of oxidative metabolism in
659 humans with insulin resistance and diabetes: Potential role of PGC1 and NRF1. *Proc Natl Acad Sci*
660 *U S A.* 2003;100(14):8466-8471. doi:10.1073/pnas.1032913100
- 661 12. Stump CS, Short KR, Bigelow ML, Schimke JM, Nair KS. Effect of insulin on human skeletal muscle
662 mitochondrial ATP production, protein synthesis, and mRNA transcripts. *Proc Natl Acad Sci U S A.*
663 2003;100(13):7996-8001. doi:10.1073/pnas.1332551100
- 664 13. Bender A, Krishnan KJ, Morris CM, et al. High levels of mitochondrial DNA deletions in substantia
665 nigra neurons in aging and Parkinson disease. *Nat Genet.* 2006;38(5):515-517.
666 doi:10.1038/ng1769
- 667 14. Taylor RW, Barron MJ, Borthwick GM, et al. Mitochondrial DNA mutations in human colonic crypt
668 stem cells Find the latest version : Mitochondrial DNA mutations in human colonic crypt stem
669 cells. *J Clin Invest.* 2003;112(9):1351-1360. doi:10.1172/JCI200319435.Introduction
- 670 15. Wanagat J, Cao Z, Pathare P, Aiken JM. Mitochondrial DNA deletion mutations colocalize with
671 segmental electron transport system abnormalities, muscle fiber atrophy, fiber splitting, and
672 oxidative damage in sarcopenia. *FASEB J.* 2001;15(2):322-332. doi:10.1096/fj.00-0320com
- 673 16. Ashar FN, Zhang Y, Longchamps RJ, et al. Association of mitochondrial DNA copy number with
674 cardiovascular disease. *JAMA Cardiol.* 2017;2(11):1247-1255. doi:10.1001/jamacardio.2017.3683
- 675 17. Calvo SE, Clauser KR, Mootha VK. MitoCarta2.0: An updated inventory of mammalian
676 mitochondrial proteins. *Nucleic Acids Res.* 2016;44(D1):D1251-D1257. doi:10.1093/nar/gkv1003
- 677 18. Schon EA, Dimauro S, Hirano M. Human mitochondrial DNA: Roles of inherited and somatic
678 mutations. *Nat Rev Genet.* 2012;13(12):878-890. doi:10.1038/nrg3275

- 679 19. Frazier AE, Thorburn DR, Compton AG. Mitochondrial energy generation disorders: Genes,
680 mechanisms, and clues to pathology. *J Biol Chem*. 2019;294(14):5386-5395.
681 doi:10.1074/jbc.R117.809194
- 682 20. Shammass MA. Telomeres, lifestyle, cancer, and aging. *Curr Opin Clin Nutr Metab Care*.
683 2011;14(1):28-34. doi:10.1097/MCO.0b013e32834121b1
- 684 21. Cawthon RM, Smith KR, O'Brien E, Sivatchenko A, Kerber RA. Association between telomere
685 length in blood and mortality in people aged 60 years or older. *Lancet*. 2003;361(9355):393-395.
686 doi:10.1016/S0140-6736(03)12384-7
- 687 22. Mizushima N, Levine B, Cuervo AM, Klionsky DJ. Autophagy fights disease through cellular self-
688 digestion. *Nature*. 2008;451(7182):1069-1075. doi:10.1038/nature06639
- 689 23. Özcan U, Cao Q, Yilmaz E, et al. Endoplasmic Reticulum Stress Links Obesity, Insulin Action, and
690 Type 2 Diabetes. *Science (80-)*. 2004;306(5695):457 LP - 461.
691 <http://science.sciencemag.org/content/306/5695/457.abstract>.
- 692 24. Kuan V, Denaxas S, Gonzalez-Izquierdo A, et al. A chronological map of 308 physical and mental
693 health conditions from 4 million individuals in the English National Health Service. *Lancet Digit*
694 *Heal*. 2019;1(2):e63-e77. doi:10.1016/s2589-7500(19)30012-3
- 695 25. Sudlow C, Gallacher J, Allen N, et al. UK Biobank: An Open Access Resource for Identifying the
696 Causes of a Wide Range of Complex Diseases of Middle and Old Age. *PLoS Med*. 2015;12(3):1-10.
697 doi:10.1371/journal.pmed.1001779
- 698 26. Teslovich TM, Musunuru K, Smith A V, et al. Biological, clinical and population relevance of 95 loci
699 for blood lipids. *Nature*. 2010;466(7307):707-713. <http://dx.doi.org/10.1038/nature09270>.
- 700 27. Ehret GB, Munroe PB, Rice KM, et al. Genetic variants in novel pathways influence blood pressure
701 and cardiovascular disease risk. *Nature*. 2011;478(7367):103-109. doi:10.1038/nature10405
- 702 28. Manning AK, Hivert M-F, Scott RA, et al. A genome-wide approach accounting for body mass
703 index identifies genetic variants influencing fasting glycemic traits and insulin resistance. *Nat*
704 *Genet*. 2012;44(6):659-669. <http://dx.doi.org/10.1038/ng.2274>.
- 705 29. Morris AP, Voight BF, Teslovich TM, et al. Large-scale association analysis provides insights into
706 the genetic architecture and pathophysiology of type 2 diabetes. *Nat Genet*. 2012;44(9):981-990.
707 doi:10.1038/ng.2383
- 708 30. Schunkert H, König IR, Kathiresan S, et al. Large-scale association analysis identifies 13 new
709 susceptibility loci for coronary artery disease. *Nat Genet*. 2011;43(4):333-340.
710 doi:10.1038/ng.784
- 711 31. Estrada K, Styrkarsdottir U, Evangelou E, et al. Genome-wide meta-analysis identifies 56 bone
712 mineral density loci and reveals 14 loci associated with risk of fracture. *Nat Genet*.
713 2012;44(5):491-501. doi:10.1038/ng.2249
- 714 32. Christophersen IE, Rienstra M, Roselli C, et al. Large-scale analyses of common and rare variants
715 identify 12 new loci associated with atrial fibrillation. *Nat Genet*. 2017;49(6):946-952.
716 doi:10.1038/ng.3843
- 717 33. Pattaro C, Teumer A, Gorski M, et al. Genetic associations at 53 loci highlight cell types and
718 biological pathways relevant for kidney function. *Nat Commun*. 2016;7:1-19.
719 doi:10.1038/ncomms10023
- 720 34. Nalls MA, Blauwendraat C, Vallerga CL, et al. Identification of novel risk loci, causal insights, and
721 heritable risk for Parkinson's disease: a meta-analysis of genome-wide association studies. *Lancet*
722 *Neurol*. 2019;18(12):1091-1102. doi:10.1016/S1474-4422(19)30320-5
- 723 35. Lambert JC, Ibrahim-Verbaas CA, Harold D, et al. Meta-analysis of 74,046 individuals identifies 11
724 new susceptibility loci for Alzheimer's disease. *Nat Genet*. 2013;45(12):1452-1458.
725 doi:10.1038/ng.2802
- 726 36. Finucane HK, Bulik-Sullivan B, Gusev A, et al. Partitioning heritability by functional annotation

- 727 using genome-wide association summary statistics. *Nat Genet.* 2015;47(11):1228-1235.
728 doi:10.1038/ng.3404
- 729 37. Bulik-Sullivan B, Finucane HK, Anttila V, et al. An atlas of genetic correlations across human
730 diseases and traits. *Nat Genet.* 2015;47(11):1236-1241. doi:10.1038/ng.3406
- 731 38. Wasmer K, Eckardt L, Breithardt G. Predisposing factors for atrial fibrillation in the elderly. *J*
732 *Geriatr Cardiol.* 2017;14(3):179-184. doi:10.11909/j.issn.1671-5411.2017.03.010
- 733 39. MacArthur J, Bowler E, Cerezo M, et al. The new NHGRI-EBI Catalog of published genome-wide
734 association studies (GWAS Catalog). *Nucleic Acids Res.* 2016;45(November 2016):gkw1133.
735 doi:10.1093/nar/gkw1133
- 736 40. Cai N, Li Y, Chang S, et al. Genetic Control over mtDNA and Its Relationship to Major Depressive
737 Disorder. *Curr Biol.* 2015;25(24):3170-3177. doi:10.1016/j.cub.2015.10.065
- 738 41. Guyatt AL, Brennan RR, Burrows K, et al. A genome-wide association study of mitochondrial DNA
739 copy number in two population-based cohorts. *Hum Genomics.* 2019;13(1):6.
740 doi:10.1186/s40246-018-0190-2
- 741 42. Ali AT, Boehme L, Carbajosa G, Seitan VC, Small KS, Hodgkinson A. Nuclear genetic regulation of
742 the human mitochondrial transcriptome. *Elife.* 2019;8:1-23. doi:10.7554/eLife.41927
- 743 43. Ali AT, Idaghdour Y, Hodgkinson A. Analysis of mitochondrial m1A/G RNA modification reveals
744 links to nuclear genetic variants and associated disease processes. *Commun Biol.* 2020;3(1):1-11.
745 doi:10.1038/s42003-020-0879-3
- 746 44. Folkersen L, Fauman E, Sabater-Lleal M, et al. Mapping of 79 loci for 83 plasma protein
747 biomarkers in cardiovascular disease. *PLoS Genet.* 2017;13(4):1-21.
748 doi:10.1371/journal.pgen.1006706
- 749 45. Jiang J, Thalamuthu A, Ho JE, et al. A meta-analysis of genome-wide association studies of growth
750 differentiation factor-15 concentration in blood. *Front Genet.* 2018;9(MAR):1-13.
751 doi:10.3389/fgene.2018.00097
- 752 46. Shin SY, Fauman EB, Petersen AK, et al. An atlas of genetic influences on human blood
753 metabolites. *Nat Genet.* 2014;46(6):543-550. doi:10.1038/ng.2982
- 754 47. Suhre K, Shin SY, Petersen AK, et al. Human metabolic individuality in biomedical and
755 pharmaceutical research. *Nature.* 2011;477(7362):54-62. doi:10.1038/nature10354
- 756 48. Raffler J, Friedrich N, Arnold M, et al. Genome-Wide Association Study with Targeted and Non-
757 targeted NMR Metabolomics Identifies 15 Novel Loci of Urinary Human Metabolic Individuality.
758 *PLoS Genet.* 2015;11(9):1-28. doi:10.1371/journal.pgen.1005487
- 759 49. Finucane HK, Reshef YA, Anttila V, et al. Heritability enrichment of specifically expressed genes
760 identifies disease-relevant tissues and cell types. *Nat Genet.* 2018;50(4):621-629.
761 doi:10.1038/s41588-018-0081-4
- 762 50. de Leeuw CA, Mooij JM, Heskes T, Posthuma D. MAGMA: Generalized Gene-Set Analysis of GWAS
763 Data. *PLoS Comput Biol.* 2015;11(4):1-19. doi:10.1371/journal.pcbi.1004219
- 764 51. Yamamoto K, Sakaue S, Matsuda K, et al. Genetic and phenotypic landscape of the mitochondrial
765 genome in the Japanese population. *Commun Biol.* 2020;3(1):104. doi:10.1038/s42003-020-0812-
766 9
- 767 52. Binder JX, Pletscher-Frankild S, Tsaou K, et al. COMPARTMENTS: Unification and visualization of
768 protein subcellular localization evidence. *Database.* 2014;2014:1-9.
769 doi:10.1093/database/bau012
- 770 53. Carbon S, Douglass E, Dunn N, et al. The Gene Ontology Resource: 20 years and still GOing
771 strong. *Nucleic Acids Res.* 2019;47(D1):D330-D338. doi:10.1093/nar/gky1055
- 772 54. Ashburner M, Ball CA, Blake JA, et al. Gene Ontology: Tool for The Unification of Biology. *Nat*
773 *Genet.* 2000;25(1):25-29. doi:10.1038/75556
- 774 55. Lambert SA, Jolma A, Campitelli LF, et al. The Human Transcription Factors. *Cell.* 2018;172(4):650-

- 775 665. doi:10.1016/j.cell.2018.01.029
- 776 56. Kapopoulou A, Mathew L, Wong A, Trono D, Jensen JD. The evolution of gene expression and
777 binding specificity of the largest transcription factor family in primates. *Evolution (N Y)*.
778 2016;70(1):167-180. doi:10.1111/evo.12819
- 779 57. Jimenez-Sanchez G, Childs B, Valle D. Human Disease Genes. *Nature*. 2001;409:853-855.
- 780 58. Worman HJ, Courvalin JC. The nuclear lamina and inherited disease. *Trends Cell Biol*.
781 2002;12(12):591-598. doi:10.1016/S0962-8924(02)02401-7
- 782 59. Cleaver JE. It was a very good year for DNA repair. *Cell*. 1994;76(1):1-4. doi:10.1016/0092-
783 8674(94)90165-1
- 784 60. Karczewski KJ, Francioli LC, Tiao G, et al. The mutational constraint spectrum quantified from
785 variation in 141,456 humans. *Nature*. 2020;581(7809):434-443. doi:10.1038/s41586-020-2308-7
- 786 61. Colacurcio DJ, Nixon RA. Disorders of lysosomal acidification—The emerging role of v-ATPase in
787 aging and neurodegenerative disease. *Ageing Res Rev*. 2016;32:75-88.
788 doi:10.1016/j.arr.2016.05.004
- 789 62. Kanfi Y, Peshti V, Gil R, et al. SIRT6 protects against pathological damage caused by diet-induced
790 obesity. *Aging Cell*. 2010;9(2):162-173. doi:10.1111/j.1474-9726.2009.00544.x
- 791 63. Blasco MA. Telomere length, stem cells and aging. *Nat Chem Biol*. 2007;3(10):640-649.
792 doi:10.1038/nchembio.2007.38
- 793 64. Bhattarai KR, Chaudhary M, Kim H-R, Chae H-J. Endoplasmic Reticulum (ER) Stress Response
794 Failure in Diseases. *Trends Cell Biol*. 2020;xx(xx):5-7. doi:10.1016/j.tcb.2020.05.004
- 795 65. De Leeuw CA, Neale BM, Heskes T, Posthuma D. The statistical properties of gene-set analysis.
796 *Nat Rev Genet*. 2016;17(6):353-364. doi:10.1038/nrg.2016.29
- 797 66. Loh PR, Bhatia G, Gusev A, et al. Contrasting genetic architectures of schizophrenia and other
798 complex diseases using fast variance-components analysis. *Nat Genet*. 2015;47(12):1385-1392.
799 doi:10.1038/ng.3431
- 800 67. Billingsley KJ, Barbosa IA, Bandrés-Ciga S, et al. Mitochondria function associated genes
801 contribute to Parkinson's Disease risk and later age at onset. *npj Park Dis*. 2019;5(1).
802 doi:10.1038/s41531-019-0080-x
- 803 68. Kraja AT, Liu C, Fetterman JL, et al. Associations of Mitochondrial and Nuclear Mitochondrial
804 Variants and Genes with Seven Metabolic Traits. *Am J Hum Genet*. 2019;104(1):112-138.
805 doi:10.1016/j.ajhg.2018.12.001
- 806 69. Jansen IE, Savage JE, Watanabe K, et al. Genome-wide meta-analysis identifies new loci and
807 functional pathways influencing Alzheimer's disease risk. *Nat Genet*. 2019;51(3):404-413.
808 doi:10.1038/s41588-018-0311-9
- 809 70. Pardiñas AF, Holmans P, Pocklington AJ, et al. Common schizophrenia alleles are enriched in
810 mutation-intolerant genes and in regions under strong background selection. *Nat Genet*.
811 2018;50(3):381-389. doi:10.1038/s41588-018-0059-2
- 812 71. Segrè A V, Consortium D, investigators M, et al. Common Inherited Variation in Mitochondrial
813 Genes Is Not Enriched for Associations with Type 2 Diabetes or Related Glycemic Traits. *PLOS*
814 *Genet*. 2010;6(8):e1001058. <https://doi.org/10.1371/journal.pgen.1001058>.
- 815 72. Saxena R, De Bakker PIW, Singer K, et al. Comprehensive association testing of common
816 mitochondrial DNA variation in metabolic disease. *Am J Hum Genet*. 2006;79(1):54-61.
817 doi:10.1086/504926
- 818 73. Hudson G, Gomez-Duran A, Wilson IJ, Chinnery PF. Recent Mitochondrial DNA Mutations
819 Increase the Risk of Developing Common Late-Onset Human Diseases. *PLoS Genet*. 2014;10(5).
820 doi:10.1371/journal.pgen.1004369
- 821 74. Hudson G, Panoutsopoulou K, Wilson I, et al. No evidence of an association between
822 mitochondrial DNA variants and osteoarthritis in 7393 cases and 5122 controls. *Ann Rheum Dis*.

- 823 2013;72(1):136-139. doi:10.1136/annrheumdis-2012-201932
- 824 75. Raule N, Sevini F, Santoro A, Altilia S, Franceschi C. Association studies on human mitochondrial
825 DNA: Methodological aspects and results in the most common age-related diseases.
826 *Mitochondrion*. 2007;7(1-2):29-38. doi:10.1016/j.mito.2006.11.013
- 827 76. Yu X, Koczan D, Sulonen AM, et al. mtDNA nt13708A variant increases the risk of multiple
828 sclerosis. *PLoS One*. 2008;3(2):1-7. doi:10.1371/journal.pone.0001530
- 829 77. Hudson G, Nalls M, Evans JR, et al. Two-stage association study and meta-analysis of
830 mitochondrial DNA variants in Parkinson disease. *Neurology*. 2013;80(22):2042-2048.
831 doi:10.1212/WNL.0b013e318294b434
- 832 78. Samuels DC, Carothers AD, Horton R, Chinnery PF. The power to detect disease associations with
833 mitochondrial DNA haplogroups. *Am J Hum Genet*. 2006;78(4):713-720. doi:10.1086/502682
- 834 79. Biffi A, Anderson CD, Nalls MA, et al. Principal-Component Analysis for Assessment of Population
835 Stratification in Mitochondrial Medical Genetics. *Am J Hum Genet*. 2010;86(6):904-917.
836 doi:10.1016/j.ajhg.2010.05.005
- 837 80. Maurano MT, Humbert R, Rynes E, et al. Systematic localization of common disease-associated
838 variation in regulatory DNA. *Science (80-)*. 2012;337(6099):1190-1195.
839 doi:10.1126/science.1222794
- 840 81. Seidman JG, Seidman C. Transcription factor haploinsufficiency: When half a loaf is not enough. *J*
841 *Clin Invest*. 2002;109(4):451-455. doi:10.1172/JCI0215043
- 842 82. Lee R Van Der, Correard S, Wasserman WW. Deregulated Regulators : Disease-Causing cis
843 Variants in Transcription Factor Genes. *Trends Genet*. 2020;xx(xx). doi:10.1016/j.tig.2020.04.006
- 844 83. Arroyo JD, Jourdain AA, Calvo SE, et al. A Genome-wide CRISPR Death Screen Identifies Genes
845 Essential for Oxidative Phosphorylation. *Cell Metab*. 2016;24(6):875-885.
846 doi:10.1016/j.cmet.2016.08.017
- 847 84. Wright S. Physiological and Evolutionary Theories of Dominance. *Am Nat*. 1934;68(714):24.
- 848 85. Kacser H, Burns JA. The molecular basis of dominance. *Genetics*. 1981;97(3-4):639-666.
- 849 86. Chance B, Williams GR. RESPIRATORY ENZYMES IN OXIDATIVE PHOSPHORYLATION: III. THE
850 STEADY STATE. *J Biol Chem*. 1955;217(1):409-428. <http://www.jbc.org/content/217/1/409.short>.
- 851 87. Vafai SB, Mootha VK. Mitochondrial disorders as windows into an ancient organelle. *Nature*.
852 2012;491(7424):374-383. doi:10.1038/nature11707
- 853 88. Balaban RS, Kantor HL, Katz LA, Briggs RW. Relation between work and phosphate metabolite in
854 the in vivo paced mammalian heart. *Science (80-)*. 1986;232(4754):1121-1123.
855 doi:10.1126/science.3704638
- 856 89. To TL, Cuadros AM, Shah H, et al. A Compendium of Genetic Modifiers of Mitochondrial
857 Dysfunction Reveals Intra-organelle Buffering. *Cell*. 2019;179(5):1222-1238.e17.
858 doi:10.1016/j.cell.2019.10.032
- 859 90. Golan D, Lander ES, Rosset S. Measuring missing heritability: Inferring the contribution of
860 common variants. *Proc Natl Acad Sci U S A*. 2014;111(49):E5272-E5281.
861 doi:10.1073/pnas.1419064111
- 862 91. Polderman TJC, Benyamin B, De Leeuw CA, et al. Meta-analysis of the heritability of human traits
863 based on fifty years of twin studies. *Nat Genet*. 2015;47(7):702-709. doi:10.1038/ng.3285
- 864 92. Fuchsberger C, Flannick J, Teslovich TM, et al. The genetic architecture of type 2 diabetes.
865 *Nature*. 2016;536(7614):41-47. doi:10.1038/nature18642
- 866 93. Hill WG, Goddard ME, Visscher PM. Data and theory point to mainly additive genetic variance for
867 complex traits. *PLoS Genet*. 2008;4(2). doi:10.1371/journal.pgen.1000008
- 868 94. Zhu Z, Bakshi A, Vinkhuyzen AAE, et al. Dominance genetic variation contributes little to the
869 missing heritability for human complex traits. *Am J Hum Genet*. 2015;96(3):377-385.
870 doi:10.1016/j.ajhg.2015.01.001

- 871 95. Rand DM, Mossman JA. Mitonuclear conflict and cooperation govern the integration of
872 genotypes, phenotypes and environments. *Philos Trans R Soc B Biol Sci.* 2020;375(1790).
873 doi:10.1098/rstb.2019.0188
- 874 96. Sackton TB, Hartl DL. Genotypic Context and Epistasis in Individuals and Populations. *Cell.*
875 2016;166(2):279-287. doi:10.1016/j.cell.2016.06.047
- 876 97. Hemani G, Shakhbazov K, Westra HJ, et al. Detection and replication of epistasis influencing
877 transcription in humans. *Nature.* 2014;508(7495):249-253. doi:10.1038/nature13005
- 878 98. Solenski NJ, DiPierro CG, Trimmer PA, Kwan AL, Helms GA. Ultrastructural changes of neuronal
879 mitochondria after transient and permanent cerebral ischemia. *Stroke.* 2002;33(3):816-824.
880 doi:10.1161/hs0302.104541
- 881 99. Flameng W, Andres J, Ferdinande P, Mattheussen M, Van Belle H. Mitochondrial function in
882 myocardial stunning. *J Mol Cell Cardiol.* 1991;23(1):1-11. doi:10.1016/0022-2828(91)90034-J
- 883 100. Weinbrenner C, Liu GS, Downey JM, Cohen M V. Cyclosporine a limits myocardial infarct size
884 even when administered after onset of ischemia. *Cardiovasc Res.* 1998;38(3):676-684.
885 doi:10.1016/S0008-6363(98)00064-9
- 886 101. Kubben N, Misteli T. Shared molecular and cellular mechanisms of premature ageing and ageing-
887 associated diseases. *Nat Rev Mol Cell Biol.* 2017;18(10):595-609. doi:10.1038/nrm.2017.68
- 888 102. Garcia CK, Wright WE, Shay JW. Human diseases of telomerase dysfunction: Insights into tissue
889 aging. *Nucleic Acids Res.* 2007;35(22):7406-7416. doi:10.1093/nar/gkm644
- 890 103. Han S, Brunet A. Histone methylation makes its mark on longevity. *Trends Cell Biol.*
891 2012;22(1):42-49. doi:10.1016/j.tcb.2011.11.001
- 892 104. Bahar R, Hartmann CH, Rodriguez KA, et al. Increased cell-to-cell variation in gene expression in
893 ageing mouse heart. *Nature.* 2006;441(7096):1011-1014. doi:10.1038/nature04844
- 894 105. Kanfi Y, Naiman S, Amir G, et al. The sirtuin SIRT6 regulates lifespan in male mice. *Nature.*
895 2012;483(7388):218-221. doi:10.1038/nature10815
- 896 106. Karczewski KJ, Dudley JT, Kukurba KR, et al. Systematic functional regulatory assessment of
897 disease-associated variants. *Proc Natl Acad Sci U S A.* 2013;110(23):9607-9612.
898 doi:10.1073/pnas.1219099110
- 899 107. Purcell S, Neale B, Todd-Brown K, et al. PLINK: A tool set for whole-genome association and
900 population-based linkage analyses. *Am J Hum Genet.* 2007;81(3):559-575. doi:10.1086/519795
- 901 108. Yanai I, Benjamin H, Shmoish M, et al. Genome-wide midrange transcription profiles reveal
902 expression level relationships in human tissue specification. *Bioinformatics.* 2005;21(5):650-659.
903 doi:10.1093/bioinformatics/bti042
- 904 109. Melé M, Ferreira PG, Reverter F, et al. The human transcriptome across tissues and individuals.
905 *Science (80-).* 2015;348(6235):660-665. <http://dx.doi.org/10.1126/science.aaa0355>.
- 906 110. Morris JA, Randall JC, Maller JB, Barrett JC. Evoker: A visualization tool for genotype intensity
907 data. *Bioinformatics.* 2010;26(14):1786-1787. doi:10.1093/bioinformatics/btq280
- 908 111. Yates AD, Achuthan P, Akanni W, et al. Ensembl 2020. *Nucleic Acids Res.* 2020;48(D1):D682-D688.
909 doi:10.1093/nar/gkz966
- 910 112. Litman T, Stein WD. Obtaining estimates for the ages of all the protein-coding genes and most of
911 the ontology-identified noncoding genes of the human genome, assigned to 19 phylostrata.
912 *Semin Oncol.* 2019;46(1):3-9. doi:10.1053/j.seminoncol.2018.11.002
913